JOC Article

Experimental and Theoretical Study of Stabilization of Delocalized Forms of Semibullvalenes and Barbaralanes by Dipolar and Polarizable Solvents. Observation of a Delocalized Structure that Is Lower in Free Energy than the Localized Form†

Maximilian Seefelder,‡ Markus Heubes,‡ Helmut Quast,*,‡ W. Daniel Edwards,§ John R. Armantrout,§ Richard Vaughan Williams,§ Christopher J. Cramer,|| Alan C. Goren,⊥ David A. Hrovat,# and Weston Thatcher Borden#

Institut für Organische Chemie der Universität Würzburg, Am Hubland, D-97074 Würzburg, Germany, Department of Chemistry, University of Idaho, Box 442343, Moscow, Idaho 83844-2343, Department of Chemistry and Supercomputer Institute, University of Minnesota, 207 Pleasant Street SE, Minneapolis, Minnesota 55455-0431, and the Departments of Chemistry, Transylvania University, Lexington, Kentucky 40508, and University of Washington, Box 351700, Seattle, Washington 98195-1700

hquast@uni-osnabrueck.de

Received February 1, 2005

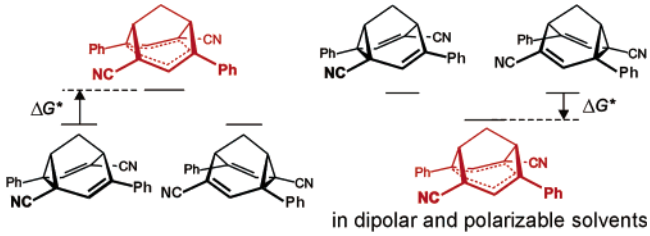

UV/vis spectra of thermochromic semibullvalenes **1** and barbaralanes **2**, which undergo rapid degenerate Cope rearrangements, display temperature-dependent shoulders (**1b**, **1d**, **1e**) or absorption maxima (**1c**, **2c**, **2f**) at the low-energy side of their strong UV bands. These long-wavelength absorptions are ascribed to Franck−Condon transitions from delocalized structures $\mathbf{1}^{deloc}$ and $\mathbf{2}^{deloc}$. Gibbs free energy differences, ΔG^*, between delocalized and localized forms were calculated from the temperature dependence of the long-wavelength absorptions. Dipolar and polarizable solvents strongly affect and even may reverse the relative stabilities of the localized and delocalized forms of **1c**, **2c**, and **2f**. For example, $\Delta G^*(\mathbf{2c}) = 8$ kJ mol^{-1} in cyclohexane, 2 kJ mol^{-1} in dimethylformamide, and −3 kJ mol^{-1} in *N*,*N*′-dimethylpropylene urea (DMPU), so that $(\mathbf{2c}^{deloc})_{DMPU}$ becomes the global minimum. In contrast to the case for **2c**, the intensities of the long-wavelength shoulders of the yellow semibullvalenes **1b**, **1d**, and **1e** are only moderately influenced by solvents, and the rates of Cope rearrangements of the nonthermochromic, colorless barbaralanes **2a** and **2b**, determined by NMR methods, are almost solvent-invariant. In search of the solute properties that are decisive in determining the influence of solvent upon ΔG^*, electrical dipole and quadrupole moments and molecular polarizabilities have been calculated using the B3LYP/6-31G* method and solvation energies have been computed with the conductorlike polarized continuum model (CPCM). The results of these calculations indicate that the solvent effects are due to the greater polarity and polarizability of the delocalized structures relative to the localized structures.

Introduction

The transition structures by which fluxional molecules[1] [e.g., bullvalene,[1,2] semibullvalene,[3] and barbaralane (**2a**)[4]] undergo rapid degenerate Cope rearrangements are electronically delocalized and bishomoaromatic. However, the successful design of a molecule in which the

† This manuscript is dedicated to Professor Waldemar Adam.

* To whom correspondence should be addressed. Current address: Hoetgerstrasse 10, D-49080 Osnabrück, Germany.
‡ Universität Würzburg.
§ University of Idaho.
|| University of Minnesota.
⊥ Transylvania University, Kentucky.
University of Washington. Current address: Department of Chemistry, University of North Texas, P.O. Box 305070, Denton, TX 76203-5070.

(1) Doering, W. v. E.; Roth, W. R. *Angew. Chem., Int. Ed. Engl.* **1963**, *2*, 115.
(2) (a) Schröder, G. *Angew. Chem., Int. Ed. Engl.* **1963**, *2*, 481. (b) Schröder, G. *Chem. Ber.* **1964**, *97*, 3140.
(3) (a) Zimmerman, H. E.; Grunewald, G. *J. Am. Chem. Soc.* **1966**, *88*, 183. (b) Zimmerman, H. E.; Binkley, R. W.; Givens, R. S.; Grunewald, G. L.; Sherwin, M. A. *J. Am. Chem. Soc.* **1969**, *91*, 3316.
(4) Doering, W. v. E.; Ferrier, B. M.; Fossel, E. T.; Hartenstein, J. H.; Jones, M., Jr.; Klumpp, G.; Rubin, R. M.; Saunders, M. *Tetrahedron* **1967**, *23*, 3943.

10.1021/jo0502089 CCC: $30.25
Published on Web 03/29/2005

neutral, bishomoaromatic structure is lower in energy than either of the two possible localized structures has proven to be elusive. Several recent review articles are devoted to this topic.[5]

Hoffmann[6] and Dewar[7,8] suggested substituents for stabilizing the transition structure for the Cope rearrangement of semibullvalene relative to the two degenerate localized structures and proposed that substituents might even reverse the relative energies of the localized and delocalized structures. Substitution of heteroatoms such as nitrogen,[7,9] phosphorus,[10] and boron carbonyl[11] for CH groups in semibullvalenes and barbaralanes has also been predicted to favor delocalized structures over localized structures. In addition, annelation strategies, which employ strain to destabilize the localized semibullvalene structures and thus to favor the delocalized geometries, have been proposed.[12,13] The relative importance of ground-state strain and bishomoaromatic stabilization in Cope transition structures of fluxional molecules has recently been analyzed.[14] Complexation of semibullvalene with the lithium cation has also been predicted to afford a delocalized system.[15] By fusing two or more barbaralanes together, delocalized C_{2v} structures become minima rather than Cope transition structures, as shown by calculations at the B3LYP/6-31G(d) level.[16]

Unfortunately, none of these strategies has yet been proven by experiment to result in a bishomoaromatic molecule in which the equilibrium geometry is fully delocalized. Moreover, since it is not possible to use either dynamic NMR spectroscopy or X-ray crystallography to differentiate unequivocally between a semibullvalene with a delocalized equilibrium geometry and one with a very low barrier to Cope rearrangement, until recently, there has been no way, even in principle, to prove experimentally that any of these strategies have, in fact, produced a semibullvalene with a fully delocalized equilibrium geometry.

The surprising thermochromism shown by dicyanosemibullvalene **1b** has been interpreted in terms of equilibrating localized and delocalized structures.[17] The corresponding Gibbs free energy difference has been calculated from variable-temperature UV/vis spectra. This well-known method is applicable, of course, when free energy differences approach zero or even become negative.[18] In this paper we provide a fuller description of the application of this method to thermochromic semibullvalenes **1** and barbaralanes **2**, described only briefly in a communication,[19] and focus on its use to probe the effects of differential solvation on the equilibrium between localized and delocalized geometries.

SCHEME 1. Degenerate Cope Rearrangements of Semibullvalenes 1 and Barbaralanes 2

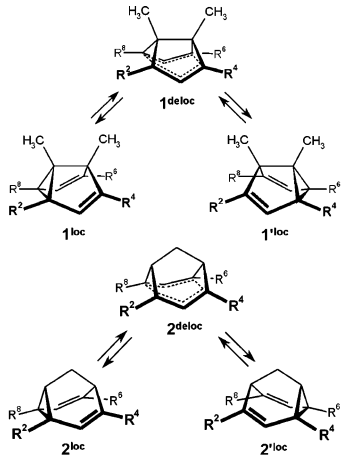

2a	$R^{2,4,6,8}$ = H	**1d, 2d**	$R^{2,4,6,8}$ = CO_2Me
1b, 2b	$R^{2,6}$ = CN, $R^{4,8}$ = H	**1e**	$R^{2,8}$ = $R^{4,6}$ = –CO–O–CO–
1c, 2c	$R^{2,6}$ = CN, $R^{4,8}$ = Ph	**2f**	$R^{2,4,6,8}$ = Ph

Increasing the dipolarity and polarizability of solvents[20] deepens the orange color of semibullvalene **1c** and barbaralanes **2c** and **2f**. This observation indicates a stabilization of the delocalized relative to the localized forms by these solvents.[21] Of special interest is our present finding that, in an *N*,*N*′-dimethylpropylene urea (DMPU) solution, delocalized barbaralane **2c**^{deloc} is favored by 3 kJ mol^{-1} over the degenerate localized structures **2c**^{loc}/**2c**′^{loc}. Thus, through a combination of substituent and solvent effects, we have now realized the goal of finding a barbaralane in which the bishomoaromatic geometry has been shown by experiments to be favored at equilibrium.

In an attempt to uncover which molecular properties cause solvation to selectively stabilize the delocalized structures in some but not all semibullvalenes and barbaralanes, we have performed B3LYP/6-31G* calculations of solvation energies using both the polarized continuum model (PCM)[22] and the conductorlike polar-

(5) (a) Williams, R. V.; Kurtz, H. A. *Adv. Phys. Org. Chem.* **1994**, *29*, 273. (b) Williams, R. V. *Adv. Theor. Interesting Mol.* **1998**, *4*, 157. (c) Williams, R. V. *Chem. Rev.* **2001**, *101*, 1185. (d) Williams, R. V. *Eur. J. Org. Chem.* **2001**, 227.

(6) Hoffmann, R.; Stohrer, W.-D. *J. Am. Chem. Soc.* **1971**, *93*, 6941.

(7) Dewar, M. J. S.; Lo, D. H. *J. Am. Chem. Soc.* **1971**, *93*, 7201.

(8) Dewar, M. J. S.; Jie, C. *Tetrahedron* **1988**, *44*, 1351.

(9) Dewar, M. J. S.; Náhlovská, Z.; Náhlovský, B. D. *J. Chem. Soc., Chem. Commun.* **1971**, 1377.

(10) Reiher, M.; Kirchner, B. *Angew. Chem., Int. Ed.* **2002**, *41*, 3429.

(11) Wu, H.-S.; Jiao H.; Wang, Z.-X.; Schleyer, P. v. R. *J. Am. Chem. Soc.* **2003**, *125*, 10524.

(12) (a) Chamot, E.; Paquette, L. A. *J. Org. Chem.* **1978**, *43*, 4527. (b) Miller, L. S.; Grohmann, K.; Dannenberg, J. J. *J. Am. Chem. Soc.* **1983**, *105*, 6862. (c) Williams, R. V.; Kurtz, H. A. *J. Org. Chem.* **1988**, *53*, 3626.

(13) Jiao, H.; Nagelkerke, R.; Kurtz, H. A.; Williams, R. V.; Borden, W. T.; Schleyer, P. v. R. *J. Am. Chem. Soc.* **1997**, *119*, 5921.

(14) (a) Brown, E. C.; Henze, D. K.; Borden, W. T. *J. Am. Chem. Soc.* **2002**, *124*, 14977. (b) Hrovat, D. A.; Brown, E. C.; Williams, R. V.; Quast, H.; Borden, W. T. *J. Org. Chem.* **2005**, *70*, 2627.

(15) Jiao, H.; Schleyer, P. v. R. *Angew. Chem., Int. Ed. Engl.* **1993**, *32*, 1760.

(16) Tantillo, D. J.; Hoffmann, R.; Houk, K. N.; Warner, P. M.; Brown, E. C.; Henze, D. K. *J. Am. Chem. Soc.* **2004**, *126*, 4256.

(17) Quast, H.; Christ, J. *Angew. Chem., Int. Ed. Engl.* **1984**, *23*, 631.

(18) Examples for the application of this method are found in reviews on thermochromic compounds: (a) Day, J. H. *Chem. Rev.* **1963**, *63*, 65. (b) Kortüm, G. *Angew. Chem.* **1958**, *70*, 14. (c) Kortüm, G. *Ber. Bunsen-Ges. Phys. Chem.* **1974**, *78*, 391. (d) Hadjoudis, E. *Mol. Spectrosc., Main Lect. Natl. Conf., 9th* **1980**, 112. (e) Ashe, A. J., III. *Adv. Organomet. Chem.* **1990**, *30*, 77. (f) Reichardt, C. *Chem. Soc. Rev.* **1992**, *21*, 147. (g) Biedermann, P. U.; Stezowski, J. J.; Agranat, I. *Eur. J. Org. Chem.* **2001**, 15.

(19) Quast, H.; Seefelder, M. *Angew. Chem., Int. Ed.* **1999**, *38*, 1064.

(20) Reichardt, C. *Solvents and Solvent Effects in Organic Chemistry*, 3rd ed.; VCH: Weinheim, Germany, 2002.

(21) Seefelder, M.; Quast, H. *Angew. Chem., Int. Ed.* **1999**, *38*, 1068.

(22) Tomasi, J.; Persico, M. *Chem. Rev.* **1994**, *94*, 2027.

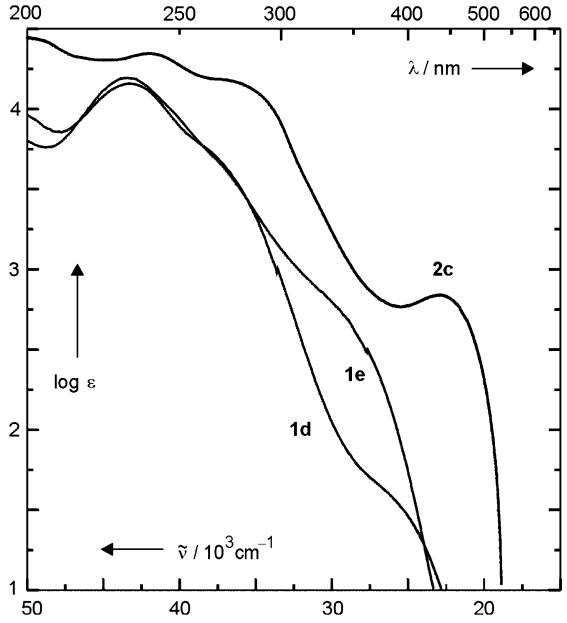

FIGURE 1. UV/vis spectra of semibullvalenes **1d** and **1e** and dicyanodiphenylbarbaralane **2c** recorded at room temperature for acetonitrile solutions.

ized continuum model (CPCM).[23] We have also computed electric dipole and quadrupole moments and molecular polarizabilities of the localized and delocalized structures. Our computational results show that, when a large increase in polarity and polarizability is predicted to accompany the change from a localized to a delocalized structure, a strong solvent dependence of the equilibrium constant is observed.

Results and Discussion

Variable-Temperature UV/Vis Spectra of Thermochromic Semibullvalenes and Barbaralanes. UV/vis spectra of the thermochromic, orange-colored semibullvalene **1c**[24] (Figure 2) and barbaralanes **2c**[25] (Figures 1 and 3) and **2f**[26] exhibit temperature-dependent long-wavelength maxima, while the spectra of the yellow semibullvalenes **1b**,[17] **1d**,[27] and **1e**[28] (Figure 1) show temperature-dependent long-wavelength shoulders that overlap with the onset of strong UV bands.

Due to the large differences in the absorbance between the long-wavelength bands and shoulders and the strong absorptions at short wavelengths, attempts at complete deconvolution of the available UV/vis spectra by standard techniques met with failure. Moreover, the majority of solvents employed, in particular the most interesting dipolar and polarizable solvents (see below), are not sufficiently transmittant[20] to allow recording of the complete UV/vis spectra. Therefore, the analysis of the UV/vis spectra had to be confined to the temperature-dependent, long-wavelength absorptions.

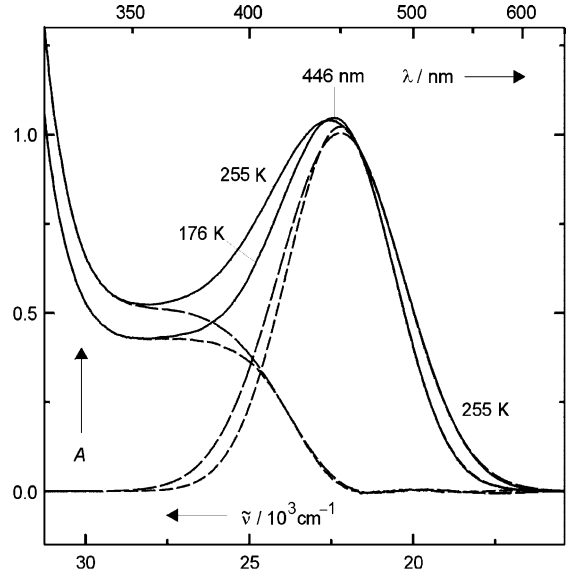

FIGURE 2. Variable-temperature UV/vis spectra (solid lines) recorded for a solution of **1c** in butyronitrile ($c = 0.769 \times 10^{-3}$ mol L^{-1}), Gaussian curves centered at $\lambda_{max}^{G} = 450$ and fitted to the low-energy side of the spectra ($\lambda \geq 470$ nm), and difference spectra obtained by subtraction of the Gaussian curves from the measured spectra (dashed lines).

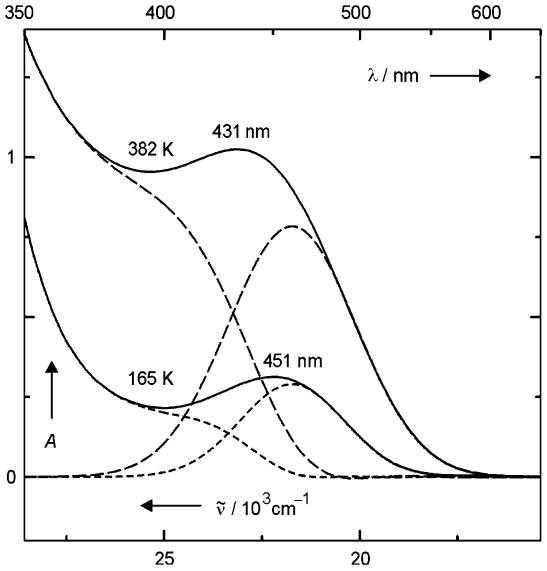

FIGURE 3. Variable-temperature UV/vis spectra (solid lines) recorded for a solution of **2c** in butyronitrile ($c = 1.25 \times 10^{-3}$ mol L^{-1}), Gaussian curves centered at $\lambda_{max}^{G} = 460$ nm and fitted to the low-energy side ($\lambda \geq 480$ nm) of the spectra, and difference spectra obtained by subtraction of the Gaussian curves from the measured spectra (dashed lines).

The long-wavelength absorption maxima of the orange-colored semibullvalene **1c** (Figure 2) and barbaralane **2c** (Figure 3) shift to the blue region with increasing temperature, and that of tetraphenylbarbaralane **2f** becomes a shoulder at the steep onset of the strong UV

(23) Barone, V.; Cossi, M. *J. Phys. Chem. A* **1998**, *102*, 1995.
(24) Quast, H.; Herkert, T.; Witzel, A.; Peters, E.-M.; Peters, K.; von Schnering, H. G. *Chem. Ber.* **1994**, *127*, 921 (the complete UV/vis spectrum is reported).
(25) Quast, H.; Geissler, E.; Herkert, T.; Knoll, K.; Peters, E.-M.; Peters, K.; von Schnering, H. G. *Chem. Ber.* **1993**, *126*, 1465.
(26) (a) Quast, H.; Knoll, K.; Peters, E.-M.; Peters, K.; von Schnering, H. G. *Chem. Ber.* **1993**, *126*, 1047 (the complete UV/vis spectrum is reported). (b) Quast, H.; Becker, C.; Peters, E.-M.; Peters, K.; von Schnering, H. G. *Liebigs Ann./Recl.* **1997**, 685.
(27) Miller, L. S.; Grohmann, K.; Dannenberg, J. J.; Todaro, L. *J. Am. Chem. Soc.* **1981**, *103*, 6249.
(28) (a) Williams, R. V.; Gadgil, V. R.; Chauhan, K.; van der Helm, D.; Hossain, M. B.; Jackman, L. M.; Fernandes, E. *J. Am. Chem. Soc.* **1996**, *118*, 4208. (b) Williams, R. V.; Gadgil, V. R.; Chauhan, K.; Jackman, L. M.; Fernandes, E. *J. Org. Chem.* **1998**, *63*, 3302.

absorption. A comparison of Figures 2 and 3 reveals that this blue shift is of greater magnitude for **2c** (9 nm/100 K) where the two bands overlap more strongly than for **1c** (2.5 nm/100 K) where there is significantly less overlap of the two bands. Obviously, these blue shifts are mainly due to the common temperature-induced broadening of the strong UV bands. Only the long-wavelength absorption of **1c**, but not that of **2c**, is sufficiently observable for an assessment of the band shape, which appears to be close to a Gaussian curve.

The presence of temperature-dependent long-wavelength UV/vis absorptions is most simply explained in terms of equilibria involving colorless localized structures and colored, less stable forms. To be able to calculate the fractions of the colored forms from integrated absorptions (and the free energy differences between the localized structures and the colored forms, see below), we assumed that the bands ascribed to the colored forms are inherently temperature-independent (except for the common temperature-induced broadening) and, thus, the integrated absorptions are measures of those fractions. In addition, we tried to minimize the effects of overlap of the long-wavelength bands with the tails of the strong UV absorptions by fitting Gaussian curves to low-energy sections of the long-wavelength bands. Attempts using Gaussian curves that were centered at the observed, temperature-dependent maxima failed to give meaningful results. Therefore, we assessed, for solutions of **1c**, **2c**, and **2f** in each solvent employed, the wavelengths of the Gaussian maxima, $\lambda_{max}{}^{G}$, from the UV/vis spectra recorded at the lowest temperature so as to yield difference spectra showing straight baselines in their long-wavelength range. These optimized values for $\lambda_{max}{}^{G}$ were also used at higher temperatures.[29]

Surprisingly, the difference spectra displayed temperature-dependent shoulders that increased with increasing temperature just as the Gaussian curves at long wavelengths do.[19] Inspection of Figure 2 indicates that the shoulder is probably not an artifact due to overlap and the necessity of fitting Gaussian curves only to a low-energy section of the bands; hence, the temperature-dependent, long-wavelength absorption of **1c** (and, probably, also of **2c** and **2f**) appears to arise from two different excitations.[30]

(29) We probed the reliability of the values for ΔG^{*} that were calculated from these Gaussian curves (Table 1) by variation of (i) the values for $\lambda_{max}{}^{G}$ and (ii) the size of the low-energy sections employed for the fit of the Gaussian curves. (i) Increasing $\lambda_{max}{}^{G}$ by 20 nm for **1c** (440→460 nm; section $\lambda \geq 470$ nm), **2c** (450→470 nm; section $\lambda \geq 480$ nm), and **2f** (455→475 nm; section $\lambda \geq 480$ nm) in butyronitrile solution resulted in an increase in ΔG^{*}, respectively, from 0.69 to 0.96, 3.09 to 3.53, and 5.35 to 5.69 kJ mol^{-1}. Increasing $\lambda_{max}{}^{G}$ by 20 nm for **2c** in dibutyl ether (448→468 nm; section $\lambda \geq 480$ nm) and DMF (458→478 nm; section $\lambda \geq 480$ nm) gave rise to an increase in ΔG^{*}, respectively, from 4.5 to 5.0 and 1.59 to 2.03 kJ mol^{-1}. (ii) Decreasing the section at the low-energy side from $\lambda \geq 470$ nm ($\lambda_{max}{}^{G} = 460$ nm) to $\lambda \geq 490$ nm ($\lambda_{max}{}^{G} = 460$ nm) for **2c** in butyronitrile solution resulted in a decrease of ΔG^{*} from 3.34 to 3.25 kJ mol^{-1}. These results indicate that errors in $\lambda_{max}{}^{G}$ of 10 nm and the variation of the chosen low-energy section by 10 nm translate into errors in ΔG^{*} of $\leq$0.3 kJ mol^{-1}.

(30) UV/vis spectra calculated at the delocalized geometry of **1c**, **2c**, and **2f** accurately reproduce the position of the longer wavelength of these two bands,[31] but the second strong transition is predicted to occur at a significantly shorter wavelength than that observed. However, several transitions with very small extinction coefficients are predicted at wavelengths between those of the two strong absorptions, and one or more of these very weak absorptions could gain intensity by vibrational borrowing (i.e., vibrationally induced mixing with the strong absorption at shorter wavelengths).

TABLE 1. Free Energy Differences ΔG^{*} (kJ mol^{-1}) between Localized Semibullvalenes and Barbaralanes and Their Colored Forms for Solutions in Butyronitrile, Integrated Extinction Coefficients ϵ_{int} (L mol^{-1} cm^{-2}), Maxima $\lambda_{max}{}^{G}$ (nm) of the Long-Wavelength Gaussian Fitting Curves, Excitation Energies ΔE_{exc} (kJ mol^{-1}) Corresponding to $\lambda_{max}{}^{G}$, and Squares of the Correlation Coefficients r^2 for the Fits of Eq 2

compd	ΔG^{*}	$10^{-6}\,\epsilon_{int}$	$\lambda_{max}{}^{G}$	ΔE_{exc}	r^2
1b	11	51[a]	360	332	1.0000
1c	0.8	25[a]	450	266	0.9997
1d	12	57	380	315	0.9998
1e	5	16	350	342	0.9982
2c	3.3	17[a]	460	260	0.9991
2f	5.5	17[a]	465	257	0.9989

[a] Values of the integrated extinction coefficients reported in ref 19 were inadvertently reported as being smaller by a factor of 10^3 than the actual values.

Experimental support for the assignment of the Gaussian curve at $\lambda_{max}{}^{G} = 460$ nm to the long-wavelength band of **2c** comes from circular dichroism spectra of (1*S*)-**2c**.[32] These spectra show a single weak, positive band with a maximum at 459 nm. This band responds to changes of temperature and solvent (see below) in the same way as the Gaussian curve fitted to the UV/vis spectrum of **2c**.

Since the UV/vis spectra of the yellow thermochromic semibullvalenes **1b**,[17] **1d**, and **1e** (Figure 1) exhibit long-wavelength shoulders rather than discrete bands, the maxima of the Gaussian curves that may represent these shoulders were estimated by visual inspection. Therefore, the calculated values for the free energy differences between the localized structures, which give rise to the UV maxima at wavelengths below 300 nm, and the sources of the yellow color are only rough estimates.

Free Energy Differences, ΔG^{*}, between Localized Semibullvalenes and Barbaralanes and Their Colored Forms. Free energy differences were calculated from integrated absorptions, A_{int}, that were obtained from the Gaussian curves described above. Consider a pair of degenerate localized structures, $\mathbf{1}^{loc}$ and $\mathbf{1}'^{loc}$, equilibrating with the colored species $\mathbf{1}^{deloc}$. The temperature dependence of the (symmetry-corrected) equilibrium constant, $K = [\mathbf{1}^{deloc}]/[\mathbf{1}^{loc}] = 2f^{*}/(1 - f^{*})$, yields eq 1, where f^{*} is the fraction of the colored species, R is the gas constant, and T is the temperature in Kelvin. The relationship, eq 2, between f^{*} and A_{int} is obtained by the Lambert−Beer Law, the validity of which has been demonstrated for **1b**[17] and **2c**[19] (ϵ_{int} in L mol^{-1} cm^{-2}, c = total concentration in mol L^{-1}, and d = path length in cm). A least-squares fit of the parameters of eq 2 to the experimental data yields the values of ΔG^{*} and ϵ_{int}. The results are listed in Table 1.

$$f^{*} = \frac{1}{1 + 2\exp(\Delta G^{*}/RT)} \quad (1)$$

$$A_{int} = \epsilon_{int} c d f^{*} = \frac{\epsilon_{int} c d}{1 + 2\exp(\Delta G^{*}/RT)} \quad (2)$$

Inspection of Table 1 reveals that the excitation energies ΔE_{exc} of the colored forms are very large compared

(31) Goren, A. C.; Hrovat, D. A.; Seefelder, M.; Quast, H.; Borden, W. T. *J. Am. Chem. Soc.* **2002**, *124*, 3469.

(32) Quast, H.; Seefelder, M.; Peters, E.-M.; Peters, K. *Eur. J. Org. Chem.* **1999**, 1811.

TABLE 2. Wavelengths λ_{max} (nm, at 298 K) of Temperature-Dependent UV/Vis Bands, Gibbs Free Energy Differences ΔG^* (kJ mol^{-1}) between Delocalized and Localized Structures in Different Solvents, and Percentages ($f^* \times 100\%$) of Delocalized Structures Calculated for a Temperature of 298 K

solvent	compd	λ_{max}	ΔG^*	$f^* \times 100\%$	compd	λ_{max}	ΔG^*	$f^* \times 100\%$
butyronitrile	**1b**		11	0.6	**1c**	442	0.8	27
dimethylformamide			9	1.2		453	0	33
cyclohexane	**2c**	436	7.9	2	**2f**		7.5[a]	3[a]
dibutyl ether		439	4.7	7				
toluene		448	4.1	9				
methanol		440	4.0	9				
benzonitrile		447	3.8	10				
acetonitrile		439	3.4	12				
butyronitrile		439	3.3	12		400[b]	5.5	5
acetone		439	2.8	14				
dimethylformamide		447	1.8	20		420[b]	2	20
dimethyl sulfoxide		453	0.4	30				
N,*N*-dimethylpropylene urea		452	−3	60		422[b]	2	20

[a] Solution in methylcyclohexane. [b] Extrapolated from spectra recorded at lower temperatures.

to free energy differences ΔG^* between localized structures and colored forms. In addition, ΔG^* values and solvent-induced changes in them (Table 2, below) are much smaller than differences between TD B3LYP/6-31G* excitation energies of localized and delocalized semibullvalenes and barbaralanes.[31] Therefore, the energy ordering of the absorption maxima, assigned to the localized semibullvalenes and barbaralanes and their colored forms, is the same for all systems irrespective of the particular solvent employed, and, most probably, also in the gas phase.

Nature of the Colored Forms of Thermochromic Semibullvalenes and Barbaralanes. Thermochromism is characteristic for semibullvalenes and barbaralanes that cross exceptionally low-energy barriers during their Cope rearrangements. This may be inferred by (i) a comparison of the yellow, thermochromic semibullvalenes **1b** and **1d**[27] with the homologous but colorless and nonthermochromic barbaralanes **2b**[17] and **2d**,[33] which possess much higher enthalpies of activation than **1b** and **1d**,[34] and (ii) the finding that exchange broadening cannot be detected at all in ^{13}C NMR spectra recorded for **1c**, **1e**, **2c**, and **2f** at the lowest accessible temperatures. Thus, the degenerate localized structures reside on very shallow ground-state energy surfaces. Increasing the temperature will take the molecular geometries to regions where the vertical excitation energies are much smaller. Combination of this feature with a well shaped excited-state surface causes long-wavelength absorptions (hot bands) to develop readily.[19,26a,35]

The yellow form of **1b** has been assigned the delocalized structure **1b**^{deloc}.[17] Likewise, the orange-colored forms of **1c**, **2c**, and **2f** were postulated to be delocalized isomers **1c**^{deloc}, **2c**^{deloc}, and **2f**^{deloc} equilibrating with the localized structures **1c**^{loc}/**1c′**^{loc}, **2c**^{loc}/**2c′**^{loc}, and **2f**^{loc}/**2f′**^{loc}, respectively.[19] This hypothesis received convincing support from (i) the excellent agreement of TD B3LYP/6-31G*-calculated vertical excitation energies of the optimized delocalized geometries of **1b**, **1c**, **2c**, and **2f** with the observed values of λ_{max}^{G}, (ii) the excellent agreement of B3LYP/6-31G*-calculated CN stretching frequencies, computed for the C_2 geometry of **1c** (= **1c**^{deloc}), with those of low-frequency CN absorptions seen in the IR spectrum of **1c**, and (iii) the finding that TD DFT-calculated vertical transitions of the localized forms **1b**^{loc}, **1c**^{loc}, **2c**^{loc}, and **2f**^{loc} occur at much shorter wavelengths (≤333 nm) than those of the delocalized forms.[31]

We probed, both computationally and experimentally, the hypothesis that the colored species may be delocalized triplets. Triplet TD DFT calculations found transitions of significant intensities at 480 and 477 nm for ^{3}**1c**^{deloc} and at 488 nm for ^{3}**2c**^{deloc}. While these maxima are quite close to the maxima of the Gaussian fitting curves (Table 1), the computed values of the energy differences between ^{3}**1c**^{deloc} and ^{1}**1c**^{deloc} (18.4 kJ mol^{-1}) and between ^{3}**2c**^{deloc} and ^{1}**2c**^{deloc} (36.8 kJ mol^{-1}) indicate that delocalized triplets are too high in energy to show the observed temperature dependence of the colored forms.

An extremely sensitive probe for paramagnetism, expected on the basis of the triplet hypothesis, is a superconducting quantum interference device (SQUID) magnetometer.[36] SQUID experiments in the temperature range 4−300 K using solid **2c** showed that the principle behavior of the sample is diamagnetic with a tiny paramagnetic contribution whose amplitude increased, however, as the temperature was lowered.[37] The opposite behavior would be expected if the orange-colored form of **2c** were the source of this signal.

EPR spectra recorded for **1b** failed to exhibit any signals. EPR spectra taken from solid **2c** at room temperature in the range 1000−3600 G showed a narrow, weak signal at 3480 G, the intensity of which increased

(33) Win, W. W.; Grohmann, K. G.; Todaro, L. *J. Org. Chem.* **1994**, *59*, 2803.

(34) Jackman, L. M.; Fernandes, E.; Heubes, M.; Quast, H. *Eur. J. Org. Chem.* **1999**, 2209 and references therein.

(35) Zilberg, S.; Haas, Y.; Danovich, D.; Shaik, S. *Angew. Chem., Int. Ed.* **1998**, *37*, 1394.

(36) (a) Clarke, J. SQUIDs: Theory and Practice. In *The New Superconducting Electronics*; Weinstock, H., Ralston, R. W., Eds.; Kluwer Academic Publishers: Dordrecht, The Netherlands, 1993. (b) Clarke, J. *Sci. Am.* **1994**, *271* (Aug), 46. (c) McElfresh, M. *Fundamentals of Magnetism and Magnetic Measurements Featuring Quantum Design's Magnetic Property Measurement System*; Quantum Design, Inc.: San Diego, CA, May 1994.

(37) A SQUID magnetometer MPMS by Quantum Design, San Diego, CA, was used. At 300 K, the amplitude of the paramagnetic contribution was ca. 2×10^{-9} JT^{-1} (on a total signal that had an amplitude of ca. 2×10^{-7} JT^{-1} at 1 T) and well above the resolution of the SQUID in the configuration employed (1×10^{-10} JT^{-1}). Thus, it was real but sufficiently small that it might be a measurement artifact. Even in the case that the signal would stem from the sample, there is no evidence that the signal was growing with the temperature.

by 55% on cooling to 77 K.[38] No half-field signal, characteristic for triplets, could be detected. A frozen dichloromethane solution of **2c** at 77 K failed to give an EPR signal.

The experimental results, as well as calculations, disprove the hypothesis that the colored forms of **1b** and **2c** might exist in the delocalized triplet state.

Influence of Solvents on Free Energy Differences between Localized and Delocalized Structures. Inspection of equally concentrated solutions of **2c** in different classes of solvents[20] at room temperature revealed that the intensity of the color varied enormously. The solution in cyclohexane had only a faint orange color, while solutions in dipolar and polarizable solvents exhibited a deep orange color, indicating the presence of substantial fractions of the colored form and thus very small ΔG^* values. Variable-temperature UV/vis spectra, recorded for a solution of **2c** in cyclohexane, afforded the highest value of ΔG^*, as anticipated on the basis of our qualitative observations. Aromatic solvents, alcohols, and nitrile solvents gave free energy differences between $\mathbf{2c}^{loc}$ and $\mathbf{2c}^{deloc}$ of $\Delta G^* = 3-5$ kJ mol^{-1}.[21] Dimethylformamide (DMF) and dimethyl sulfoxide (DMSO) resulted in a substantial further lowering of ΔG^* (Table 2). The relative areas under the Gaussian curves, employed in the deconvolution of the spectra of **2c** that were taken in hexamethylphosphoramide, dimethylacetamide, and *N*-methylpyrrolidinone turned out to be almost temperature-invariant, thus suggesting that $\Delta G^* \approx 0$ in these solvents.

The finding of greatest interest was that solutions of **2c** in the highly dipolar and polarizable solvent *N*,*N*′-dimethylpropylene urea (DMPU) showed a clear *reversal* of the usual temperature dependence of the integrated absorbance. The relative intensity of the long-wavelength band decreased with increasing temperature (Figure 4).

The fit of the parameters of eq 2 to the A_{int} vs T data revealed that, in solutions in DMPU, $\mathbf{2c}^{deloc}$ is more stable by 3 kJ mol^{-1} than $\mathbf{2c}^{loc}$. This value is in satisfactory agreement with the value of $\Delta G^* = -2$ kJ mol^{-1}, estimated from a ^{13}C NMR study of deuterium-labeled **2c**, using an extension of Saunders' isotopic perturbation method.[39] These two independent measurements both agree that $\mathbf{2c}^{deloc}$ is the global energy minimum in DMPU. The dramatic influence of solvents on the free energy difference ΔG^* between $\mathbf{2c}^{loc}$ and $\mathbf{2c}^{deloc}$ may be visualized by plots showing the temperature dependence of the percentage ($f^* \times 100\%$) of $\mathbf{2c}^{deloc}$ in different solvents (Figure 5).[40]

The unexpected finding that the relative stabilities of $\mathbf{2c}^{loc}$ and $\mathbf{2c}^{deloc}$ are strongly solvent-dependent prompted

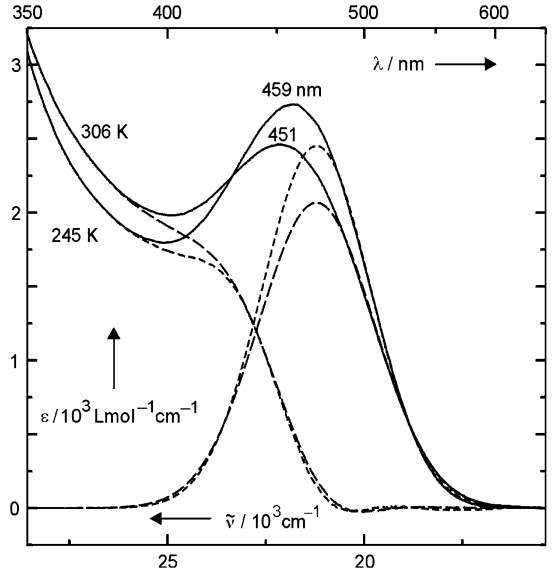

FIGURE 4. Variable-temperature UV/vis spectra (solid lines) recorded for a solution of dicyanodiphenylbarbaralane **2c** in *N*,*N*′-dimethylpropylene urea, Gaussian curves centered at 471 nm and fitted to the low-energy side of the spectra ($\lambda \geq 480$ nm), and difference spectra obtained by subtraction of the Gaussian curves from the spectra (dashed lines).

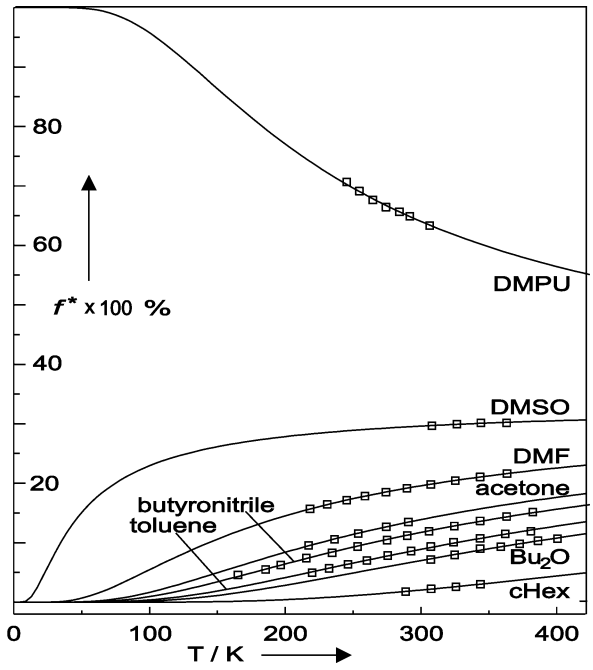

FIGURE 5. Percentages ($f^* \times 100\%$) of delocalized barbaralane $\mathbf{2c}^{deloc}$ in different solvents versus temperature (K). The curves through the data points were calculated with eq 1 using the ΔG^* value obtained for the solvent.

measurement of variable-temperature UV/vis spectra for solutions of **1b**, **1c**, and **2f**, albeit in a limited number of solvents. DMF as a solvent appears to lower the value of ΔG^* for dicyanosemibullvalene **1b** by 20% compared to butyronitrile.

The results obtained for solutions of **1c** and **2f** resemble those obtained for **2c**. Unfortunately, the thermal rearrangement of dicyanodiphenylsemibullvalene **1c** to cyclooctatetraenes[41] limits the study of its thermochromism

(38) EPR spectra were taken on a Bruker ESP 300 X-band EPR spectrometer. For measurements of **2c** at 77 K, a finger-shaped Dewar flask filled with liquid nitrogen was inserted into the microwave cavity. The observed EPR signal had a width of ca. 30 G and did not show any fine structure. Besides a doublet radical impurity, electron exchange between two molecules in the crystal may have caused the EPR signal.

(39) Quast, H.; Seefelder, M.; Becker, C.; Heubes, M.; Peters, E.-M.; Peters, K. *Eur. J. Org. Chem.* **1999**, 2763; *corrigendum* **2000**, 691.

(40) Selective stabilization by dipolar and polarizable solvents of $\mathbf{2c}^{deloc}$, relative to $\mathbf{2c}^{loc}$, suggests that the separation between the long-wavelength band attributed to $\mathbf{2c}^{deloc}$ and the shorter-wavelength absorption due to $\mathbf{2c}^{loc}$ should decrease in these solvents. Unfortunately, the wavelength of the latter (cf. Figure 1) could not be measured due to a lack of sufficiently transparent dipolar and polarizable solvents and overlap with absorptions of the phenyl chromophores.

TABLE 3. Rate Constants k (s^{-1}) of Cope Rearrangements of Barbaralanes 2a and 2b as Calculated from Exchange Broadenings of Signals in 150.9 MHz ^{13}C NMR Spectra Recorded in the Limits of Fast (217 and 280 K) and Slow Exchange (167 K)

	2a		**2a**		**2b**	
solvent	$10^{-6}\,k_{280}$	k_{rel}	k_{167}	k_{rel}	$10^{-6}\,k_{217}$	k_{rel}
[D_{14}]methylcyclohexane	4.52	1.00	320	1.00		
[D_4]methanol	4.78	1.06				
chlorodifluoromethane/[D_6]dimethyl ether (3:1)	4.84	1.07	380	1.19	5.36	1.00
[D_6]acetone	4.95	1.10	487	1.52	5.56	1.04
[D_8]tetrahydrofuran	5.20	1.15	509	1.59		
[D_8]toluene	5.23	1.16	547	1.71	6.27	1.17
carbon tetrachloride	5.38	1.19				
[D_3]acetonitrile	5.49	1.21				
[D_7]dimethylformamide	5.59	1.24			7.17	1.34
[D_{18}]hexamethylphosphoramide	5.59	1.24				
dimethylacetamide	5.61	1.24				
[D_5]pyridine	5.87	1.30				
[D]chloroform	6.37	1.41				

to temperatures below ca. 250 K. For a solution of **1c** in DMF in the temperature range of 218−251 K, the integrated absorbance ascribed to **1c**^{deloc} is temperature-invariant within ±0.5%, corresponding to $\Delta G^* \approx 0$. We note that the influence of dipolar and polarizable solvents on the free energy difference between **1c**^{loc} and **1c**^{deloc} accords well with the observed increase in the intensity of low-frequency IR nitrile bands of **1c**, ascribed to **1c**^{deloc}, in media of increasing polarity.[31]

Solvents influence the energy difference between **2f**^{loc} and **2f**^{deloc}, but less so than for **2c**. In particular, DMPU does not reverse the relative energies of **2f**^{loc} and **2f**^{deloc}, as it does in the case of **2c**^{loc} and **2c**^{deloc}. The results of the studies of the effects of solvents on the UV/vis spectra of **1b**, **1c**, **2c**, and **2f** are summarized in Table 2.

The influence of solvents on UV/vis spectra of the yellow semibullvalenes **1b**, **1d**, and **1e** (see Supporting Information) was investigated at a constant temperature of 303 ± 2 K. The solvent effects on the weak shoulders in the spectra of **1b** and **1d** are small. Dipolar and polarizable solvents enhance the shoulder in the spectra of **1b** and thus indicate a slight increase of the fraction of **1b**^{deloc}, while a similar trend cannot be seen in the spectra of **1d**. The temperature-dependent shoulder in the spectra of **1e** is somewhat more strongly influenced by solvents than in the spectra of **1b** and **1d**. Surprisingly, dipolar and polarizable solvents appear to decrease the size of the long-wavelength shoulder, which is ascribed to **1e**^{deloc}.

It was intriguing to probe the influence of solvents on the relative free energies ΔG^* of the delocalized and localized structures for nonthermochromic barbaralanes **2a** and **2b**. Since their delocalized forms (**2**^{deloc}) are presumably the transition structures for the Cope rearrangements **2**^{loc} ⇌ **2′**^{loc}, the rate constants for this reaction might reflect solvent effects on free energy differences ΔG^* between localized and delocalized structures. Although rates of Cope rearrangements have been determined for many barbaralanes and semibullvalenes, usually only a single solvent has been employed.[1,4,33,34] We measured exchange broadenings in ^{13}C NMR spectra of **2a** and **2b** for a number of different solvents at very accurately determined temperatures.[42] These temperatures were chosen to achieve optimal signal-to-noise ratios and half-widths. Rate constants were calculated from the exchange broadenings in the limits of fast and slow exchange and are listed in Table 3 in the order of increasing values.

Each of the three sets of data in Table 3 is influenced by solvents in the same way. This finding argues against the hypothesis that the observed solvent effects might be due to different temperature dependences of the ^{13}C chemical shifts in different solvents. Table 3 shows that solvents do influence the rate constants, but very little. The variations in rate translate into changes in Gibbs free energies of activation of no more than 0.8 kJ mol^{-1}. The near-independence of the measured rate constants from solvent is reassuring, because a host of different solvents have been employed in previous rate studies on similar compounds.

The experimental results described in this section allow us to classify semibullvalenes and barbaralanes according to how solvents influence the relative free energies of their delocalized and localized forms. The influence of dipolar and polarizable solvents on selectively stabilizing the delocalized structure is strong for **1c**, **2c**, and **2f**, at most moderate for **1b** and **1d**, and almost negligible for **2a** and **2b**. **1e** exhibits mild solvent dependency with the delocalized form appearing to be favored by the less polar solvents.

In an attempt to understand the solvent properties that cause the dramatic effects on **2c**, two of us have previously correlated the ΔG^* values obtained for **2c** in 21 different solvents[21] with three of the four parameters in the equation devised by Abraham, Kamlet, and Taft (eq 3),[43] viz. a solvatochromic parameter, π^*, which describes a combination of dipolarity and polarizability, the proton-donating ability, α, and the electron pair-donating ability, β. The first term in eq 3 is the ΔG^* value (kJ mol^{-1}), extrapolated for saturated hydrocarbon solvents, whose parameters are all defined as zero. The values of the coefficients are small, as expected in view of the small absolute size of the solvent effects. The parameter π^* has the largest coefficient, followed by the coefficient for β. Increases in these two parameters result in smaller values for ΔG^*(**2c**).

$$\Delta G^*(\mathbf{2c}) = 6.7 - 3.8\pi^* + 1.5\alpha - 2.6\beta \qquad (3)$$

(41) Quast, H.; Heubes, M.; Dietz, T.; Witzel, A.; Boenke, M.; Roth, W. R. *Eur. J. Org. Chem.* **1999**, 813.

(42) Quast, H.; Heubes, M.; Dunger, A.; Limbach, H.-H. *J. Magn. Reson.* **1998**, *134*, 236.

Calculations. To try to understand why the term for solvent dipolarity and polarizability has the largest coefficient in eq 3, we used electronic structure calculations to compute the dipole and quadrupole moments and the molecular polarizabilities of the localized and delocalized geometries of **1b**, **1c**, **1e**, **2a**−**c**, and **2f**. We also performed polarized continuum model (PCM)[22] and conductorlike polarized continuum model (CPCM)[23] calculations in an attempt to quantify the relative magnitudes of electrostatics, dispersion, and other contributions to differential solvation of the localized and delocalized geometries of these semibullvalenes and barbaralanes.

Calculations of the Energy Difference between 1e^{loc} and 1e^{deloc} and the Excitation Energy of 1e^{deloc}. While the results of B3LYP/6-31G* calculations on semibullvalenes **1b** and **1c** and barbaralanes **2a**−**c** and **2f** have already been published,[31,44] the results of DFT calculations on semibullvalene bisanhydride (**1e**) have not previously been reported. B3LYP/6-31G*-optimized geometries, energies, and thermal corrections for **1e**^{deloc} are available in the Supporting Information.

B3LYP calculations found no localized energy minimum for bisanhydride **1e**. All B3LYP geometry optimizations led to a delocalized geometry. However, ab initio HF/6-31G* optimizations of the geometry of **1e** provided energy minima, corresponding to the localized forms, **1e**^{loc} and **1e**$'^{loc}$, and also located the transition structure **1e**^{deloc} connecting them. At the HF level, the delocalized C_{2v}-symmetric species **1e**^{deloc} was found to be 31.4 kJ mol^{-1} higher in enthalpy than **1e**^{loc}. These results are essentially identical to those obtained using the larger 6-311G** basis set and validate the use of the 6-31G* basis set for the current study.[45]

As is also the case with AM1 calculations,[28] at the HF/6-31G* level the localized forms **1e**^{loc} and **1e**$'^{loc}$ are calculated to be lower in energy than **1e**^{deloc}. It is well-known that the HF method overestimates bond localization in aromatics and that the inclusion of electron correlation is essential to accurately represent such systems.[46] The necessity of including both static and dynamic electron correlation in calculations on the Cope rearrangement has been amply demonstrated.[47]

In contrast to HF calculations, B3LYP/6-31G* studies on Cope rearrangements, including those of semibullvalenes and barbaralanes, have furnished geometries and relative energies in reasonable agreement with experiment.[13,31,44,48] However, for semibullvalenes **1b** and **1c** and barbaralanes **2c** and **2f**, B3LYP/6-31G* calculations tend to overestimate the relative stabilities of the delocalized species and to give energy differences between delocalized and localized species that are too low by 8−12 kJ mol^{-1}.[31,44] This seems also to be the case for **1e**.[49] Single-point B3LYP/6-31G* calculations at the HF stationary points for **1e**^{loc} and **1e**^{deloc} resulted in the symmetric species **1e**^{deloc} being computed to be *lower* in energy than the corresponding localized structures, **1e**^{loc} and **1e**$'^{loc}$, by 8.7 kJ mol^{-1}.

Although these results could mean that bishomoaromatic structure **1e**^{deloc} is the only energy minimum in the gas phase, the following points argue against this conclusion: (a) in the crystalline state, **1e**^{loc} is the species that is observed;[45] (b) the monoethyl homologue of **1e** has a localized structure in solution;[51] and (c) the temperature dependence of the intensity of the long-wavelength shoulder in the UV/vis spectrum of **1e** indicates that in butyronitrile, **1e**^{deloc} is ca. 5 kJ mol^{-1} higher in energy than **1e**^{loc} (Table 1). Therefore, it seems more likely that B3LYP tends to overestimate the stability of **1e**^{deloc} relative to **1e**^{loc} and **1e**$'^{loc}$. This overestimation is apparently sufficiently large in size to eliminate any barrier between them on the B3LYP potential energy surface, so that there is only a single minimum on this PES, corresponding to the delocalized structure.[52]

The electronic excitation energies for **1e** were computed at the TD B3LYP level[53] using both the B3LYP- (**1e**^{deloc}) and HF-optimized (**1e**^{loc}) geometries. The value of λ_{max} = 359 nm, calculated at the former geometry, is in better agreement with the experimental value of λ_{max} = 350 nm (Table 1) than is the value of λ_{max} = 270 nm, computed at the latter geometry. As is the case for **1b**, **1c**, **2c**, and **2f**,[31] the TD DFT calculations on **1e** suggest that the temperature- and solvent-dependent, long-wavelength absorption seen in the UV/vis spectra of this semibullvalene (Figure 1) belong to the delocalized species (**1e**^{deloc}).

Differences in Electric Dipole Moments, Quadrupole Moments, and Electrostatic Solvation Free Energies between Localized and Delocalized Geometries. The tendency for polar solvents to stabilize some delocalized semibullvalene and barbaralane structures, relative to the localized alternatives, could derive from the former structures being more polar than the latter. To assess this possibility, we first computed the electric dipole and quadrupole moments of these various structures.

For these uncharged molecules, the magnitude of the dipole moment is independent of the choice of origin, but this is not true of the quadrupole moment. Therefore, we

(43) Abraham, M. H.; Grellier, P. L.; Abboud, J.-L. M.; Doherty, R. M.; Taft, R. W. *Can. J. Chem.* **1988**, *66*, 2673 and references therein.

(44) Hrovat, D. A.; Williams, R. V.; Goren, A. C.; Borden, W. T. *J. Comput. Chem.* **2001**, *22*, 1565.

(45) Williams, R. V.; Gadgil, V. R.; Luger, P.; Koritsanszky, T.; Weber, M. *J. Org. Chem.* **1999**, *64*, 1180.

(46) Williams, R. V.; Edwards, W. D.; Vij, A.; Tolbert, R. W.; Mitchell, R. H. *J. Org. Chem.* **1998**, *63*, 3125.

(47) Borden, W. T.; Davidson, E. R. *Acc. Chem. Res.* **1996**, *29*, 67.

(48) (a) Hrovat, D. A.; Beno, B. R.; Lange, H.; Yoo, H.-Y.; Houk, K. N.; Borden, W. T. *J. Am. Chem. Soc.* **1999**, *121*, 10529. (b) Hrovat, D. A.; Chen, J.; Houk, K. N.; Borden, W. T. *J. Am. Chem. Soc.* **2000**, *122*, 7456.

(49) The tendency of many modern DFT functionals to overestimate the stability of highly delocalized electronic structures compared to more localized ones is attributed to errors in the electronic self-interaction correction: (a) Ref 50. (b) Lim, M. H.; Worthington, S. E.; Dulles, F. J.; Cramer C. J. In *Chemical Applications of Density Functional Theory*; Laird, B. B., Ross, R. B., Ziegler, T., Eds.; ACS Symposium Series 629; American Chemical Society: Washington, DC, 1996; Vol. 629, p 402. (c) Bally, T.; Sastry, G. N. *J. Phys. Chem. A* **1997**, *101*, 7923.

(50) Cramer, C. J. *Essentials of Computational Chemistry: Theories and Models*; Wiley: Chichester, UK, 2002.

(51) Heubes, M.; Dietz, T.; Quast, H.; Seefelder, M.; Witzel, A.; Gadgil, V. R.; Williams, R. V. *J. Org. Chem.* **2001**, *66*, 1949.

(52) In contrast to B3LYP calculations on **1e**, reported in this work, B3PW91 calculations *do* predict a triple-minimum PES, with almost degenerate localized and delocalized structures, and the gas-phase electron-diffraction data for **1e** could be fitted by any one of three models, a localized structure, a delocalized structure, or a mixture of the two: Samdal, S.; Richardson, A. D.; Hedberg, K.; Gadgil, V. R.; Meyer, M. M.; Williams, R. V. *Helv. Chim. Acta* **2003**, *86*, 1741.

(53) (a) Bauernschmitt, R.; Ahlrichs, R. *Chem. Phys. Lett.* **1996**, *256*, 454. (b) Casida, M. E.; Jamorski, C.; Casida, K. C.; Salahub, D. *J. Chem. Phys.* **1998**, *108*, 4439. (c) Stratmann, R. E.; Scuseria, G. E.; Frisch, M. J. *J. Chem. Phys.* **1998**, *109*, 8218.

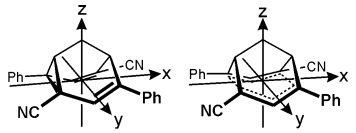

FIGURE 6. Drawings of the oriented structures **2c**^{loc} (left) and **2c**^{deloc} (right) showing the coordinate axes.

TABLE 4. B3LYP/6-31G* Calculated Electric Dipole Moments μ (10^{-30} C m) and Mean Quadrupole Moments Θ (10^{-40} C m^2) and Changes in Them that Result from Transition from Localized to Delocalized Structures[a]

compd	μ^{loc} [b]	μ^{deloc} [b]	$\Delta\mu$[c]	Θ^{loc} [d]	Θ^{deloc} [d]	$\Delta\Theta$[e]
almost no influence of solvents on relative stability						
2a	1.3	0.3	−1.1	173.6	174.2	0.6
2b	8.4	9.5	1.1	279.0	278.8	−0.2
weak influence of solvents on relative stability						
1b	5.2	6.0	0.8	298.2	298.6	0.4
1e	10.9[f]	12.5[f]	1.6	409.8[f]	409.7[f]	−0.1
		13.1			413.5	
strong influence of solvents on relative stability						
1c	4.2	5.5	1.3	499.7	496.6	−3.1
2c	6.9	7.2	0.3	479.7	475.7	−4.0
2f	1.2	0.0	−1.2	602.6	601.5	−1.1

[a] Compounds are grouped according to the effect that solvents have on the relative stabilities of the localized and delocalized forms. [b] $\mu = [(\mu_x)^2 + (\mu_y)^2 + (\mu_z)^2]^{1/2}$. [c] $\Delta\mu = \mu^{deloc} - \mu^{loc}$. [d] Mean quadrupole moment $\Theta = (|\Theta_{xx}| + |\Theta_{yy}| + |\Theta_{zz}|)/3$. [e] $\Delta\Theta = \Theta^{deloc} - \Theta^{loc}$. [f] RHF geometry.

specify our choice of coordinates. All molecules were oriented so that the origin of the coordinate axes was at the center of the mean plane of carbon atoms C2, C4, C6, and C8. The *x*,*y* plane is orthogonal to the C_2 symmetry axis, where one exists. Note that the *x*,*z* plane is the symmetry plane in **1e**^{loc}, **1e**^{deloc}, **2a**^{loc}, **2a**^{deloc}, **2f**^{loc}, and **2f**^{deloc}, and the positive *x* and *z* directions bisect the internuclear distances C4−C6 and C1−C5, respectively, of these molecules. An example of this orientation of the axes is shown in Figure 6 for **2c**.

The calculated dipole and quadrupole moments are given in Table 4. Inspection of this Table reveals that the transition from localized to delocalized structures changes the dipole moment magnitudes by up to 2×10^{-30} C m. However, there is no correlation between the calculated changes in dipole moments, some of which are positive and some of which are negative, and the effects of solvents on the relative energies of the two structures. Similarly, the trace of the quadrupole moment tensor remains constant to within less than 1%, and the molecules that are most sensitive to solvents actually show the greatest calculated decreases in quadrupole moments.

Unfortunately, there is no guarantee in molecules of the size of those in Table 4 that the overall polarity will be well represented by an electric multipole expansion, truncated at low order. For example, one difference between the delocalized and localized structures could be that the four substituents in series **c**, **d**, **e**, and **f** more effectively withdraw electrons in the delocalized structure than in the localized structure. Such an effect would not be revealed until consideration of the octapole moments.

Rather than carry out further analyses of a possibly slowly convergent series of multipolar expansions, we assessed the polarity difference between localized and delocalized structures directly by computation of their interactions with their own reaction field within the context of the polarized continuum solvent models, PCM[22] and CPCM.[23] Since these models make use of the continuous charge distribution from the wave function, they effectively carry out the multipolar expansion to infinite order.

Table 5 gives the CPCM free energies calculated at the B3LYP/6-31G*//RHF/6-31G* level of theory. The results obtained from calculations at the B3LYP/6-31G* geometries are qualitatively similar and are given in Supporting Information. Because an equilibrium geometry for **1e**^{loc} does not exist at this level of theory, B3LYP/6-31G*-optimized geometries could not be used for PCM or CPCM calculations on **1e**.

The data in Table 5 include the electrostatic free energies of solvation for both the frozen (i.e., gas-phase) charge distribution and for the relaxed charge distribution that is equilibrated with the reaction field. The first row of entries for each compound is for the frozen charge distribution. Comparison of the second row with the first shows the effect of the field, due to the solvent, on increasing the solvation free energies by polarizing the solute.

Inspection of the data in Table 5 reveals that changing the solvent from cyclohexane to DMSO is calculated to selectively stabilize the delocalized geometries of all the molecules in the table. However, the size of this solvent effect on the energy differences between the localized and delocalized geometries of **1b**, **1e**, **2a**, and **2b** is predicted to be negligible. This computational result is consistent with the small solvent sensitivities that are observed for these compounds experimentally.

The small effect of changing the solvent dipolarity on the energy difference between the localized and delocalized geometries of **1b**, **1e**, **2a**, and **2b** is due to the small absolute effect that solvation has on this energy difference. Among these four molecules, the largest effect of solvation on this difference is predicted for **2b**. However, going from the gas phase to DMSO is predicted to change the energy difference between **2b**^{loc} and **2b**^{deloc} by only 0.6 kJ mol^{-1}.

On the other hand, for systems **1c**, **2c**, and **2f**, the absolute solvation effects on the energy difference between the localized and delocalized geometries range to as high as 3.2 kJ mol^{-1} for **2c** in DMSO, and differential solvation effects of 1 to 2 kJ mol^{-1} are predicted for **1c** and **2c** on going from cyclohexane to DMSO. In these two molecules the differential solvation effects between cyclohexane and DMSO increase by 25−56% when relaxation of the electronic wave function is taken into account. Particularly in these two molecules, the delocalized structures are not only more polar than the localized structures: the delocalized structures are also more polarizable. Therefore, the polarity difference between localized and delocalized structures is enhanced upon allowing relaxation of the gas-phase wave function.[54]

The magnitude of the calculated difference between cyclohexane and DMSO on preferentially stabilizing the delocalized geometry of **2c** is, at most, about 25% of the measured difference of 7.5 kJ mol^{-1}, given in Table 2. Solvent dipolarity, at least as measured by the dielectric constant (which is the only solvent property that enters

TABLE 5. CPCM Electrostatic Solvation Free Energies (kJ mol^{-1}) of Localized and Delocalized Forms of 1b, 1c, 1e, 2a−c, and 2f in Cyclohexane and DMSO and the Differences between These Free Energies[a]

	Cyclohexane			DMSO			
compd	loc	deloc	$\Delta^{loc\rightarrow deloc}$	loc	deloc	$\Delta^{loc\rightarrow deloc}$	$\Delta^{cHex\rightarrow DMSO}$
almost no influence of solvents on relative stability							
2a	−2.2[b]	−2.4	−0.2	−4.3	−4.6	−0.3	−0.1
	−2.4[c]	−2.5	−0.2	−4.6	−4.9	−0.3	−0.1
2b	−12.6	−12.8	−0.2	−24.3	−24.8	−0.5	−0.3
	−13.4	−13.7	−0.3	−27.8	−28.4	−0.6	−0.3
weak influence of solvents on relative stability							
1b	−10.3	−10.4	−0.1	−19.9	−20.1	−0.2	−0.1
	−10.9	−11.0	−0.1	−22.5	−22.7	−0.2	−0.1
1e	−13.6	−13.7	−0.1	−26.3	−26.5	−0.2	−0.1
	−14.2	−14.4	−0.2	−28.7	−28.7	−0.3	−0.1
strong influence of solvents on relative stability							
1c	−11.9	−13.2	−1.3	−23.0	−25.5	−2.5	−1.2
	−12.6	−14.0	−1.4	−25.8	−28.7	−2.9	−1.5
2c	−14.2	−15.5	−1.3	−27.6	−30.0	−2.4	−1.1
	−15.1	−16.6	−1.5	−31.2	−34.4	−3.2	−1.7
2f	−7.3	−7.8	−0.5	−14.1	−15.0	−0.9	−0.4
	−7.6	−8.1	−0.5	−15.2	−16.2	−1.0	−0.5

[a] CPCM solvation free energies are based on B3LYP/6-31G*//RHF/6-31G* calculations. [b] Top row of numbers for each compound refers to gas-phase frozen electrostatic free energy of solvation, computed as $\langle\Psi(gas)|V[\Psi(gas)]|\Psi(gas)\rangle$ where $V[\Psi(gas)]$ is the reaction field operator in solution, computed from $\Psi(gas)$, the gas-phase wave function. [c] Bottom row of numbers refers to relaxed electrostatic free energy of solvation, computed as $\langle\Psi(sol)|V[\Psi(sol)]|\Psi(sol)\rangle$ where $V[\Psi(sol)]$ is the reaction field operator in solution, computed from $\Psi(sol)$, the solution-phase wave function.

into a continuum solvation calculation), is apparently not the only way that solvent affects the free energy difference between localized and delocalized structures.

This conclusion can be drawn directly from the experimental data without recourse to any calculations. Table 2 indicates that in methanol, which has a dielectric constant of $\epsilon = 32.7$, ΔG^* for **2c** is 4.0 kJ mol^{-1}, whereas in DMPU, which has a very similar dielectric constant of $\epsilon = 36.1$, ΔG^* for **2c** is −3 kJ mol^{-1}. Effects, other than solvent dielectric, must be responsible for this difference between methanol and DMPU on the relative free energies of **2c**^{loc} and **2c**^{deloc}. Nevertheless, the CPCM free energy of solvation does provide a useful means to calculate the electrostatic components of solvation free energies.

For solvents such as cyclohexane that have very small dielectric constants, it has been suggested that the conductorlike approximation in CPCM[23] may lead to an overestimation of polarization free energies.[55] In such cases, it may be more accurate to employ the dielectric formulation, contained in the PCM.[22,56]

We have, in fact, carried out PCM calculations for all of the molecules in Table 5.[57] Indeed, we do find that the calculated sizes of the effects of cyclohexane solvation on the gas-phase free energy differences between the localized and delocalized geometries of **1c** and **2c** are reduced, compared to the sizes of the effects that are computed by CPCM. This reduction in the size of the calculated cyclohexane solvation effects leads to the calculated differences between the cyclohexane and DMSO solvation effects being larger when computed by PCM rather than by CPCM. However, the magnitude of the increase is only about 0.5 kJ mol^{-1} for each molecule.

Thus, an upper limit to the calculated effect of the difference between the dielectric constants of cyclohexane and DMSO on relative free energies of the localized and delocalized geometries of **1c** and **2c** is certainly no more than 3 kJ mol^{-1}. The experimental data in Table 2 show that this upper limit is considerably less than half of the measured effect that this change in solvents has on the free energy difference between **2c**^{loc} and **2c**^{deloc}.

Effects of Differences in Polarizabilities between Localized and Delocalized Structures on Differential Dispersion Energies. As discussed in the preceding section, molecular polarizability contributes indirectly to the electrostatic component of solvation free energy by affecting the degree to which the solvent can polarize the electrons of the solute and thus increase charge separation in the solute. However, molecular polarizability plays a more direct role in determining the magnitude of dispersion interactions between the solute and the solvent. These London forces come from electrostatic interactions between the mutually induced dipole moments of the solute and the solvent,[59] which are produced by the quantum mechanical correlation of the motions of

(54) This observation suggests that also permitting *geometric relaxation* (i.e., reoptimizing the geometry with the reaction field turned on) might provide a still larger differential solvation effect. However, many studies have shown that the magnitude of additional solvation free energy that is typically associated with geometric relaxation is only about 10% of the frozen-geometry solvation free energy: Cramer, C. J.; Truhlar, D. G. *Chem. Rev.* **1999**, *99*, 2161. Therefore, we estimate that, even after geometry reoptimization, the differential solvation effect between cyclohexane and DMSO on selectively stabilizing the delocalized structure would increase to at most 2 kJ mol^{-1} for **1c** and **2c** and to certainly no more than 1 kJ mol^{-1} for **2f**.

(55) Klamt, A.; Schürmann, G. *J. Chem. Soc., Perkin Trans. 2* **1993**, 799.

(56) Miertus, S.; Scrocco, E.; Tomasi, J. *Chem. Phys.* **1981**, *55*, 117.

(57) PCM is much more sensitive than CPCM to the numerical instabilities, associated with a renormalization step, which must be carried out for solute charge that lies outside of the solute cavity in the continuum solvent (so-called charge penetration): (a) Ref 58. (b) Chipman, D. M. *J. Chem. Phys.* **1997**, *106*, 10194. (c) Cossi, M.; Rega, N.; Scalmani, G.; Barone, V. *J. Chem. Phys.* **2001**, *114*, 5691. (d) Chipman, D. M. *J. Chem. Phys.* **2002**, *116*, 10129. In some of the least polar semibullvalenes and barbaralanes (e.g., **2a**), this instability leads to results that are clearly nonphysical. Therefore, the equivalent of Table 5, based on PCM, is not given here, but such a table is available in Supporting Information.

their electrons. Therefore, the sizes of the dispersion interactions between solute and solvent depend on the polarizabilities of both types of molecules.

The quantum mechanical calculation of dispersion is not trivial. Dispersion is included in the calculated interaction energies between two molecular fragments only if the level of electronic structure theory used takes adequate account of dynamical electron correlation.[47] Unfortunately, most DFT functionals (e.g., B3LYP) do not satisfactorily describe dispersion interactions. MP2 calculations could be used, but they would be rather expensive for the large solutes and the solvents in Table 2, particularly if the entire first solvation shell were included and its very high-dimensional configurational space were properly sampled. Therefore, we have not attempted to compute the effects of dispersion interactions on the differences between the solvation free energies of the localized and delocalized geometries of **1** and **2**.[60] However, we can make some qualitative observations about the effects of dispersion interactions on these differential solvation free energies.

In his original formulation, London derived eq 4 for the dispersion energy, U_{disp}, between two molecules.[59]

$$U_{disp} = -\frac{3\alpha_1\alpha_2}{2r^6}\left(\frac{IP_1IP_2}{IP_1 + IP_2}\right) \quad (4)$$

In this equation, r is the distance between molecules 1 and 2, which have polarizabilities α and ionization potentials IP. If we take molecule 1 to be the solute and molecule 2 to be the solvent, and we consider the change in dispersion energy associated with the transformation from a localized to a delocalized geometry, eq 4 becomes

$$\Delta U_{disp}^{loc\rightarrow deloc} = -\left(\frac{3\alpha_{solv}IP_{solv}}{2r^6}\right)\left(\frac{\alpha^{deloc}}{1+\frac{IP_{solv}}{IP^{deloc}}} - \frac{\alpha^{loc}}{1+\frac{IP_{solv}}{IP^{loc}}}\right) \quad (5)$$

If we assume that the IPs for the localized and delocalized structures are sufficiently close to one another to be treated as a constant, viz. $IP^{loc/deloc}$, eq 5 simplifies to

$$\Delta U_{disp}^{loc\rightarrow deloc} \approx -\left[\frac{3\alpha_{solv}}{2r^6\left(\frac{1}{IP_{solv}} + \frac{1}{IP^{loc/deloc}}\right)}\right](\alpha^{deloc} - \alpha^{loc}) \quad (6)$$

Equation 6 makes two qualitative predictions about the effects of polarizability on the difference between the dispersion energies of the localized and delocalized geometries. First, if the polarizability of the delocalized structure is greater than that of the localized structure, dispersion will favor the former over the latter, and the difference between the dispersion energies of the two structures will depend linearly on the difference between their polarizabilities. Second, the difference between the dispersion energies associated with the two geometries will increase linearly in magnitude with increasing polarizability of the solvent.

TABLE 6. B3LYP/6-31G* Calculated Polarizabilities (10^{-40} C^2 m^2 J^{-1}) and the Changes (Δ) in Them that Result on Transition from Localized to Delocalized Structures[a]

compd	α^{loc} [b]	α^{deloc} [b]	$\Delta\alpha$ [c]	$\Delta\alpha_{xx}$ [d]	$\Delta\alpha_{yy}$ [d]	$\Delta\alpha_{zz}$ [d]
almost no influence of solvents on relative stability						
2a	13.3	14.2	0.9	0.7	1.9	0.1
2b	18.7	21.1	2.4	3.5	3.4	0.3
weak influence of solvents on relative stability						
1b	20.6	22.8	2.2	3.5	3.3	−0.09
1e	21.3[e]	22.5[e] 23.6	1.2	1.9	1.7	−0.1
strong influence of solvents on relative stability						
1c	41.7	48.5	6.8	12.5	6.6	1.4
2c	41.0	48.5	7.5	14.3	8.6	−0.6
2f	57.4	66.7	9.3	18.7	10.5	−1.2

[a] Compounds are grouped according to the effect that solvents have on the relative stabilities of the localized and delocalized forms [b] Mean polarizability $\alpha = (\alpha_{xx} + \alpha_{yy} + \alpha_{zz})/3$. [c] $\Delta\alpha = \alpha^{deloc} - \alpha^{loc}$. [d] Changes of the principal components $\Delta\alpha_{ii} = \alpha_{ii}^{deloc} - \alpha_{ii}^{loc}$. [e] RHF geometry.

With respect to the first point, we have computed the polarizabilities of the localized and delocalized forms of **1b**, **1c**, **1e**, **2a**−**c**, and **2f** (Table 6). In each case the delocalized species is more polarizable than the localized species. It is noteworthy that the largest differences in polarizability between the localized and delocalized geometries are calculated for the three phenyl-substituted compounds **1c**, **2c**, and **2f**. These compounds also have the largest absolute polarizabilities due to the roughly linear relationship between molecular volume and polarizability; however, it is the *change* in polarizability that matters in eq 6. This equation leads to the prediction that **1c**, **2c**, and **2f** should be the compounds that are most sensitive to changes in solvent polarizability, with the delocalized geometry of each being increasingly stabilized, relative to the localized geometry, as the polarizability of the solvent increases.

A simple measure of solvent polarizability is provided by the index of refraction n.[20] Some of the solvents in Table 2 that have the lowest n are methanol (1.328),[61] acetonitrile (1.344), and dibutyl ether (1.399). Dibutyl ether also has a very small dielectric constant ($\epsilon = 3.08$), so it is not surprising that dibutyl ether perturbs ΔG^* relatively little compared to cyclohexane, for which ΔG^* is the greatest. Methanol and acetonitrile are both considerably more polar ($\epsilon = 32.7$ and 35.9, respectively) than dibutyl ether; therefore, they exert an additional, presumably electrostatic, effect on ΔG^*.

Solvents with large n include DMPU (1.488), toluene (1.497), and benzonitrile (1.528). DMPU combines a large value of n with a large dipolarity ($\epsilon = 36.1$), so its position in Table 2 as the solvent that most stabilizes $\mathbf{2c}^{deloc}$ over $\mathbf{2c}^{loc}$ is wholly consistent with our analysis. Toluene has a very low dipolarity ($\epsilon = 2.38$) and can only exert an

(58) Cossi, M.; Rega, N.; Scalmani, G.; Barone, V. *J. Comput. Chem.* **2003**, *24*, 669.

(59) London, F. *Z. Physik* **1930**, *63*, 245.

(60) CPCM does include a dispersion contribution to the total free energy of solvation. However, the model employed to estimate that contribution depends on the atomic composition of the solute and not on its electronic wave function. Thus, the model is not suitable for computing changes in the dispersion energy that derive from changes in polarizability between the localized and delocalized geometries of **1** and **2**.

(61) All indices of refraction refer to 293 K at the wavelength of the sodium D line.

influence through polarizability. Consequently, its effect on ΔG^*, relative to ΔG^* in cyclohexane, is only about one-third of the effect of DMPU.

Curiously, Table 2 shows that benzonitrile gives only a slightly higher value of ΔG^* than toluene, even though the former solvent ($\epsilon = 25.2$) is much more dipolar than the latter. This finding suggests that, in addition to solvent dipolarity and polarizability, other factors also play a role in the effects of solvents on the free energy difference between the localized and delocalized geometries of **2c**.[20,22,62]

Scrutiny of the principal components of the polarizability tensors of **1c**, **2c**, and **2f** in Table 6 reveals that significant changes occur only in the *x*,*y* plane and not along the *z* axis. The largest changes are along the *x* axis, which is parallel to the allyl groups in the delocalized structures and to the phenyl groups that are conjugated with the allyls. This extended conjugation in the delocalized forms of **1c**, **2c**, and **2f** is responsible for these three delocalized species having the highest polarizabilities. This conjugation is, of course, also responsible for the long-wavelength UV/vis absorptions and for the low energies of $\mathbf{1c}^{deloc}$, $\mathbf{2c}^{deloc}$, and $\mathbf{2f}^{deloc}$ relative to the localized geometries.

Conclusion

Calculation of relative free energies from variable-temperature UV/vis spectra of thermochromic semibullvalenes and barbaralanes revealed that the relative stabilities of the delocalized form ($\mathbf{2c}^{deloc}$) and the degenerate localized structures ($\mathbf{2c}^{loc}$ and $\mathbf{2c'}^{loc}$) of dicyanodiphenylbarbaralane **2c** range from $\Delta G^* = 7-8$ kJ mol^{-1} in saturated hydrocarbons to ca. -3 kJ mol^{-1} in *N*,*N*′-dimethylpropylene urea. Thus, through a combination of substituent and solvent effects, the goal of converting a Cope transition structure, viz. that of the parent barbaralane ($\mathbf{2a}^{deloc}$), into the global energy minimum $(\mathbf{2c}^{deloc})_{solv}$ has been achieved for the first time.

B3LYP-calculated values of solvation free energies, using CPCM, and of molecular polarizabilities indicate that the higher polarity and polarizability of $\mathbf{2c}^{deloc}$, compared to $\mathbf{2c}^{loc}$ and $\mathbf{2c'}^{loc}$, is largely responsible for the observed solvent dependence of the relative free energies of the localized and delocalized structures. The computational results are consistent with the experimental finding that the largest factor in eq 3, for the properties of solvents that effect selective stabilization of $\mathbf{2c}^{deloc}$ by solvation, is the term for solvent polarity and polarizability.

We expect that similar dependencies of the relative free energies of localized and delocalized species will be observed for other molecules that have shallow ground-state energy surfaces involving localized and delocalized structures of different polarities and polarizabilities. Calculations may prove to be a convenient way of predicting whether these are sufficiently different for solvation to have a large effect on the relative stabilities.

Experimental Section

Source of Material. The semibullvalenes **1b**,[63] **1c**,[24] **1d**,[28b] and **1e**[28b] and the barbaralanes **2a**,[64] **2b**,[65] **2c**,[25] and **2f**[26b] have been prepared as described in the literature.

Variable-Temperature UV/Vis Spectra were recorded on degassed solutions at precisely defined temperatures that were measured inside of the 1 cm quartz cells. Particular care was taken in these experiments to ensure that the changes in the spectra with temperature were completely reversible and thus not due to decomposition of the sample. Thermal expansion of the solutions was accounted for with the help of density data for the pure solvents (standard temperature 298 K).

Computational Methods. Molecular geometries were optimized at both the Hartree−Fock (HF) and density functional (DFT) levels of theory using the 6-31G* basis set.[5,66] We employed the hybrid B3LYP functional,[67] which combines Becke's gradient-corrected exchange functional[68] with the gradient-corrected functional of Lee, Yang, and Parr.[69] Analytic computation of the molecular vibrational frequencies was carried out to confirm the nature of all stationary points and to compute thermal contributions to enthalpies and free energies.[50,66]

Electronic excitation energies were computed using time-dependent (TD) DFT with the B3LYP functional.[53] Continuum solvation calculations were carried out for 298 K cyclohexane ($\epsilon = 2.02$) and DMSO ($\epsilon = 46.45$),[20] employing the PCM[22] and CPCM[23] methods. The default united-atom solute cavity was used.[58] All TD DFT and continuum solvation calculations employed geometries optimized in the gas phase. The calculations were carried out with either the Gaussian 98[70] or Jaguar 4.0[71] program suites.

Acknowledgment. We express our gratitude to Professor Laurens Molenkamp, Dr. Charles Gould, and Dr. Georg Schmidt, Physik-Department der Universität Würzburg, for performing and interpreting the SQUID experiments, and to Professor Georg Gescheidt and Dr.

(62) (a) If the molecular volumes of the localized and delocalized geometries were significantly different, the larger would be increasingly disfavored in solvents with increasing surface tensions by its larger cavitation energy. However, we compute the two geometries to have molecular volumes that are identical to within 1% or so, and using scaled-particle theory (Ref 23. Pierotti, R. A. *Chem. Rev.* **1976**, *76*, 717), differences between the cavitation energies in cyclohexane and DMSO are predicted to amount to at most 0.2 kJ mol^{-1} for any pair of localized and delocalized structures. (b) Other possible effects include solute/solvent charge transfer, hydrogen bonding, and Lewis acid/Lewis base interactions. The magnitudes of the coefficients of α and β in eq 3 suggest that such effects do indeed play a role in determining ΔG^* and that the combined sizes of these effects may be similar to those of solvent polarity and polarizability. Attempts to model computationally the effects of charge transfer, hydrogen bonding, and Lewis acid/Lewis base interactions would require inclusion of explicit solvent molecules in the calculations.

(63) Quast, H.; Mayer, A. *Liebigs Ann. Chem.* **1988**, 1155.
(64) Quast, H.; Dietz, T.; Peters, E.-M.; Peters, K.; von Schnering, H. G. *Liebigs Ann.* **1995**, 1159.
(65) Quast, H.; Görlach, Y.; Stawitz, J.; Peters, E.-M.; Peters, K.; von Schnering, H. G. *Chem. Ber.* **1984**, *117*, 2745.
(66) Hehre, W. J.; Radom, L.; Schleyer, P. v. R.; Pople, J. A. *Ab Initio Molecular Orbital Theory*; Wiley: New York, 1986.
(67) (a) Becke, A. D. *J. Chem. Phys.* **1993**, *98*, 5648. (b) Stephens, P. J.; Devlin, F. J.; Chabalowski, C. F.; Frisch, M. J. *J. Phys. Chem.* **1994**, *98*, 11623.
(68) Becke, A. D. *Phys. Rev. A* **1988**, *38*, 3098.
(69) Lee, C.; Yang, W.; Parr, R. G. *Phys. Rev. B* **1988**, *37*, 785.
(70) *Gaussian 98*, revisions A6 and A9. Frisch, M. J.; Trucks, G. W.; Schlegel, H. B.; Scuseria, G. E.; Robb, M. A.; Cheeseman, J. R.; Zakrzewski, V. G.; Montgomery, J. A., Jr.; Stratmann, R. E.; Burant, J. C.; Dapprich, S.; Millam, J. M.; Daniels, A. D.; Kudin, K. N.; Strain, M. C.; Farkas, O.; Tomasi, J.; Barone, V.; Cossi, M.; Cammi, R.; Mennucci, B.; Pomelli, C.; Adamo, C.; Clifford, S.; Ochterski, J.; Petersson, G. A.; Ayala, P. Y.; Cui, Q.; Morokuma, K.; Malick, D. K.; Rabuck, A. D.; Raghavachari, K.; Foresman, J. B.; Cioslowski, J.; Ortiz, J. V.; Stefanov, B. B.; Liu, G.; Liashenko, A.; Piskorz, P.; Komaromi, I.; Gomperts, R.; Martin, R. L.; Fox, D. J.; Keith, T.; Al-Laham, M. A.; Peng, C. Y.; Nanayakkara, A.; Gonzalez, C.; Challacombe, M.; Gill, P. M. W.; Johnson, B. G.; Chen, W.; Wong, M. W.; Andres, J. L.; Head-Gordon, M.; Replogle, E. S.; Pople, J. A.; Gaussian, Inc.: Pittsburgh, PA, 1998.
(71) *Jaguar 4.0*; Schrödinger, Inc.: Portland, Oregon, 2000.

Daniela Hristova, Institute of Physical and Theoretical Chemistry, Graz University of Technology, Austria, for recording and interpreting the EPR spectra. We thank the National Science Foundation for generously supporting this research at the Universities of Minnesota (Grant No. CHE-0203346) and Washington. A.C.G. would like to thank Transylvania University for supporting a sabbatical leave at the University of Washington and the National Computational Science Alliance for use of the HP N-4000 Complex at the University of Kentucky. H.Q. and R.V.W. express their gratitude for a NATO Collaborative Research Grant (No. CRG 973044).

Supporting Information Available: Instrumentation and recording of VT UV/vis spectra, properties of solvents, calculation of integrated absorbance, and λ_{max}(298 K) for **1c** and **2c** in different solvents, VT UV/vis spectra of **1b**−**e**, **2c**, and **2f**, line widths in ^{13}C NMR spectra of **2a** and **2b**, optimized geometries, energies, and thermal corrections for **1e**, dipole moments, quadrupole moments, and molecular polarizabilities for **1b**, **1c**, **1e**, **2a**−**c**, and **2f**, CPCM electrostatic solvation free energies for **1b**, **1c**, **1e**, **2a**−**c**, and **2f** calculated at the B3LYP/6-31G* geometries, PCM electrostatic solvation free energies for **1b**, **1c**, **1e**, **2a**−**c**, and **2f** based on B3LYP/6-31G*//RHF/6-31G* calculations, and triplet TD DFT calculated excitation energies for ^{3}**1c**^{deloc} and ^{3}**2c**^{deloc}. This material is available free of charge via the Internet at http://pubs.acs.org.

JO0502089